Detection, in situ recognition of coarse root systems using ground penetrating radar (GPR)

Mingkai Wang, Jian Wen*, Wenbin Li and Zhaoxi Li

***Abstract*—**The growth of coarse tree root systems is extremely complex as well as the cross-growth in three dimensions is very difficult, it is clear that the quantitative recognition and the observation are difficult to detect in situ. Previously, coarse tree root systems are usually detected by destructive methods such as excavation and profiling. In this paper, we used ground penetrating radar (GPR) to detect coarse root systems according to the GPR principle that forming clear hyperbolic reflections on the GPR radargram when electromagnetic waves travel across two surfaces with different dielectric constants. First, we use GprMax 3.0 to simulated the hyperbola of root reflection with different root directions based on finite-different time-domain method (FDTD).Then, the coordinates of coarse root systems are readily inversed by Symmetry Algorithm and Hough Transform. To demonstrate the viability of two algorithms, the inversion of coordinates is compared with the actual coordinates in the forward condition and the relative error is obtained. Furthermore, the detection and in situ recognition of the coarse tree root systems can achieved in the simulation experiment and field experiment. The results show that the root localization is quite accurate. Research results can also provide a solid basis for the three-dimensional reconstruction of ancient and famous trees and intersecting trees, as well as nondestructive testing means in the safety maintenance of trees.

***Keywords*—**coarse root systems, in situ recognition, Symmetry Algorithm, Hough Transform.

I. Introduction

Coarse root systems, which are responsible for most root carbon storage, play a significant role in plant ecosystem functioning as they transfer water and nutrient [1]. But the study of coarse root system is not profound enough because of the difficulty of underground observation and sampling. Meanwhile, traditional methods have many disadvantages in a large number of experiments [2]. Thus, non-destructing testing (NDT) methods are becoming popular for the root system testing [3], due to their high efficiency and overall reliability of the information produced [4]. Among these techniques, the ground penetrating radar (GPR) is particularly imports that based on the scattering of electromagnetic waves that are radiated from a transmitting antenna [2-4]. Further, according to the difference of the electrical parameters between root and surrounding soils, the hyperbolic diffraction parameters (two-way time delay, amplitude areas, pixels within the threshold range, mean pixel intensity and reflector tally, etc.) were formed to locate the roots, evaluate the biomass and draw the root configuration [5-7].

Currently, the great achievements have been made in the field of root detection, such as the root biomass detection and the automatic 3D reconstruction of roots [5-20]. Fang et al described a root growth system in which the roots grow in a solid gel matrix that was used to reconstruct 3D root architecture in situ and dynamically simulate [19]. Liu et al build a functional relationship between the hyperbolic signal and relevant parameters of the root orientation based on the principle of EM wave propagation [21]. Zhu et al establish a feasible detection method to delineate the root distributions from the acquired 3D data by 3D GPR, and propose some reasonable indexes for estimating root biomass (including the biomass of a single root and total biomass in the specific depth ranges) in field conditions [13]. In a word, there is no doubt that the importance of the spatial distribution of roots in GPR detection. Furthermore, these researches have analyzed the influence of roots system spatial distribution on radar waves [15].

In some ways, the use of GPR for root detection seems to be maturing. However, the previous work on the detection of tree roots using ground-penetrating radar has indicated that there are many limiting factors that included dielectric constants of soil and roots, the direction and diameter of roots, and the spatial distribution of roots [22-23]. Moreover, they rarely consider the direction of the coarse root systems. The spatial distribution of roots is the problem that has received the most attention among these factors as there are many branches of the tree, and the cross-growth in three dimensions is very difficult [24].

Under these conditions thereupon, the emphasis of this paper is to study the GPR signal characteristics of tree root and in situ identification of its roots. To this purpose, we build many different forward models to simulate real situations, as well as inversed the GPR data obtained from a simulation experiment and a controlled experiment in the field. Surely, the results can provide theoretical basis and knowledge carrier for in situ identification of tree roots, meanwhile, it can provide theoretical basis and knowledge carriers for the theoretical studies of root system biology, forestry and underground

This research is financially supported by the National Natural Science Foundations of China (Grant No.31600589).

Mingkai Wang, with Beijing Forestry University, Beijing, 100083 China (corresponding author to provide e-mail:misslittlesheep@163.com).

Jian Wen, with Beijing Forestry University, Beijing, 100083 China (corresponding author to provide e-mail: wenjian@bjfu.edu.cn).

Wenbin Li, with Beijing Forestry University, Beijing, 100083 China(e-mail: leewb@bjfu.edu.cn)

Zhaoxi Li, with Beijing Forestry University, Beijing, 100083 China (e-mail: lizhaoxi14@163.com).

ecology.

To achieve this aim, this paper is divided into four parts. First, we put forward a mathematical model about signal hyperbola and received the forward image of coarse root systems in different orientations with the use of GPRMax 3.0 [25]. Then, we obtained the location of the vertex of root profile hyperbola by the Symmetric Algorithm and Hough Transform. Lastly, we can identify and locate the GPR hyperbola where exist root in simple level, combining control experiment with a field experiment.

II. Procedure For Paper Submission

A. Simulation Experiment Of Different Root Orientation

In natural conditions, roots generally develop in a radial pattern, with the taproot centered and tilted slightly downward owing to its geotropism [26]. Thus, the root systems are going to grow at different angles. The root orientation can been described by two parameters in the coordinate system: the horizontal orientation angle α and the vertical inclination angle β, as shown in Fig.1 [21]. The vertical inclination β is defined as the angle of the projection of the root onto the y-z plane and z-axis. The azimuth angle α is defined as the acute angle between the projection of the buried root onto the ground plane (x–z plane) and the direction of the scanning line of the GPR [27].

Next, we built the above models with GPRMax 3.0 that a GPR signal simulating software, to create simulated data [25]. The model boundary lengths were 0.24m and 0.20m and the scan number was 60 [28]. The dx, dy and dz (PML boundary condition)were all 0.002m. The root center was in the center of the model, and the root direction changes as the root rotate. The dielectric constant permittivity of the soil and the root respectively were 5 and 10. The root was set in the form of cylinders with diameters of 0.01 m. That worth mentioning that the center frequency of the radar is 900MHZ means that the depth to been detected needs to be less than 0.5m. The depth we have choice is reasonable [29].

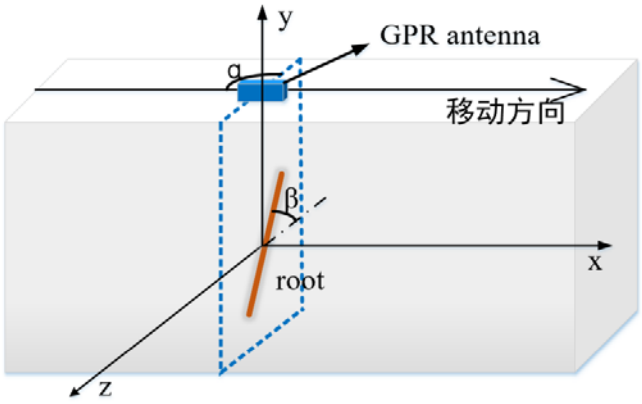

Fig. 1 Illustration of the root orientation in spatial rectangular coordinate system.

In our experiment, the time window was set to 3 ns [29], and the step of the antenna in per scan number was 0.002 m. In addition, the radar transmitter was placed in the 0.02 m and the radar receiver in 0.06 m. Based on these factors, we obtained radar reflection images in different directions of the root. These images can really well simulate the scene of different root directions.

Additionally, the simulated images need to visualized by the imaging command in MATLAB and underwent imagery preprocessing [7] (first arrival time pickup, temperature shift error correction, background removal, gaining, and signal-to-noise ratio evaluation) to enhance the quality of the images.

B. GPR Hyperbolic Mathematical Model

When the radar that is sent and received in parallel is close to the ground or almost close to, let's make an assumption that the propagation path in the soil that is homogeneous medium becomes relatively simple that only reflected back to the receiving antenna after the target. The projection point of a target on a radar detection line is x_0 as shown in Fig.2 [30]. In addition, the t_0 is a two-way travel time of x_0. The velocity of the wave is constant for the reason that homogeneous medium. According to the triangle Pythagorean Theorem, the hyperbola is represented by the following equation:

$$(z_i)^2 - (x - x_0)^2 = (z_0)^2 \tag{1}$$

Obviously, $z_0 = v \cdot t_0 / 2, z_i = v \cdot t_i / 2$

Therefore, the formula (1) becomes:

$$\frac{(t_i)^2}{(t_0)^2} - \frac{(x-x_0)^2}{\left(v \cdot \frac{t_0}{2} + r\right)^2} \tag{2}$$

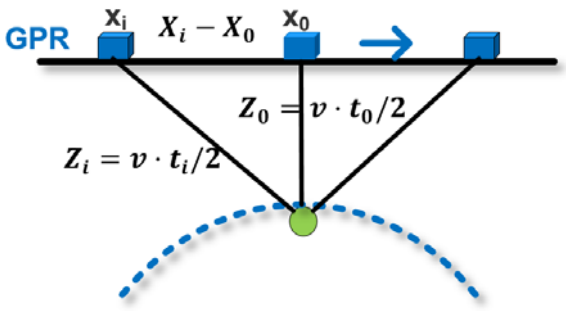

(a)

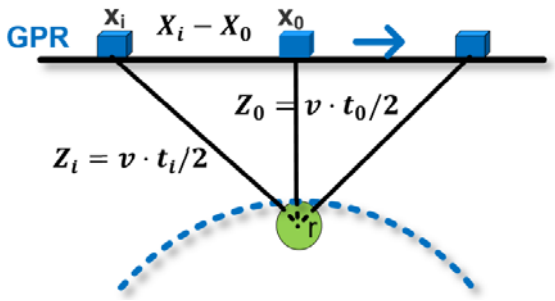

(b)

Fig 2 (a) Hyperbola model under ideal conditions, (b) Hyperbola model in the presence of target radius.

You can see that the time delay of target conforms to the constraint equation of the standard hyperbola from equation (2). However, the diameter of a tree's root system can not be ignored in most experiments. As well as, the GPR wave propagation path will change as shown in Fig. 2(b), so the formula (1) transform into:

$$(z_i + r)^2 - (x - x_0)^2 = (z_0 + r)^2 \quad (3)$$

Finally, put the z_i and z_0 in in the equation (3):

$$\frac{(t_i+\frac{2r}{v})^2}{(t_0+\frac{2r}{v})^2} - \frac{(x-x_0)^2}{\left(v\cdot\frac{t_0}{2}+r\right)^2} = 1 \quad (4)$$

Similarly, it fit with the constraint equation ($\frac{x^2}{a^2} - \frac{y^2}{b^2} = 1$) of the standard hyperbola from in the function (4). In other words, the signal presents a hyperbolic model because of the ellipse characteristic of root. Actually, the hyperbola contains the information of electromagnetic wave velocity and dielectric constant of medium. So we need to pay attention to this point.

C. Symmetry Algorithm And Hough Transform Algorithm

The vertex coordinates of hyperbolic can obtained from Symmetry Algorithm that based on the principle that the target hyperbolic signal is symmetric about the vertex and shows a monotone decreasing trend on both sides of the vertex. Symmetry curve equation can been indicated as [31-32]:

$$S(j) = \sum_{i=1}^{ysize} \sum_{m=1}^{k} |f[i, j-m] - f[i, j+m]| \quad (5)$$

The f [i, j] is pixels of two-dimensional scan image get from GPR. The image array is defined by ysize and k.

Moreover, the procedure for extracting the vertices of the GPR hyperbola as follows:

1) removal the direct wave of GPR image use Matgpr [33-34].

2) judge the extreme point of the GPR hyperbola, the number of extremum points is the same as the number of roots when the symmetry curves is not intersect, or otherwise, we need analyze if the intersection of the Symmetry curve match the characteristics of the root or not.

3) get the minimum point of Symmetry Curve use Matlab algorithm:

$$[m, n] = \min[S(j)] \quad (6)$$

m is indicated as the horizontal position of hyperbola vertex.

4) extract A-scan where the hyperbola vertex is located after extracting the horizontal position of hyperbola vertex. The maximum energy of the target echo in the ROI is the time delay direction coordinate of the hyperbolic vertex [31].

Then, the electromagnetic wave velocity in the medium should be known for the extraction of root hyperbolic vertex. In order to gain electromagnetic wave velocity by Hough Transform, there is the preprocessor that extract the hyperbolic. That is needed to extract the contour of the hyperbola. We can get a focal point in the parameter space on the basis of point-line duality of Hough Transform. As far as the value of the focus point can represent the accuracy of electromagnetic wave velocity estimation, we can extract the velocity information from the hyperbola. So in order to do that, we first have to transform the equation of the hyperbola as depicted in Fig.3(a):

$$(\frac{v}{2} \times \Delta t \times y)^2 = [(x - x_0) \times \Delta x]^2 + (\frac{v}{2} \times \Delta t \times y_0)^2 \quad (7)$$

And the final transform is given by (8):

$$U = -K(x) \times V + x \quad (8)$$

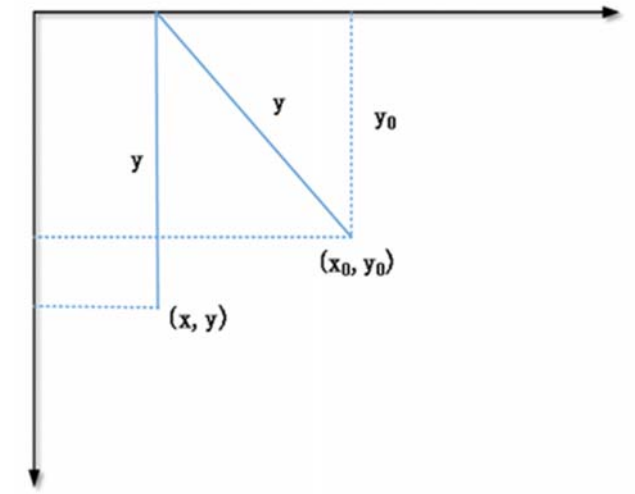

(a)

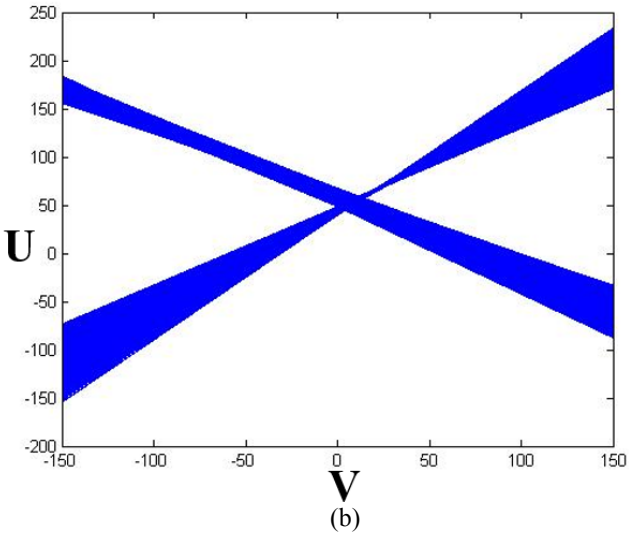

(b)

Fig. 3 (a) the mathematical form of the Hough Transformation of a hyperbola, (b) the form of the hyperbola in the V-U domain of the Hough Transform.

Among in the (8),

$$V = \frac{1}{M} = \frac{(v \times \Delta t)^2}{(4 \times \Delta x)^2} \quad (9)$$

$$U = x_0 \quad (10)$$

$$K(x) = -\dot{y}(x) \times y(x) \quad (11)$$

So we can get one y'(x) as long as we take a point on the GPR B-scan graph, as a result, it's a lot easier to get K(x). Meanwhile, there's going to be a line with a slope of -K(x) and an intercept of x that in the V-U domain of the Hough Transform as shown in the Fig.3(b). As well as, the V can be indicted as the intersection of many straight lines in the hough coordinate system. Thus, the electromagnetic velocity v can been calculated by formula (9) [34-35].

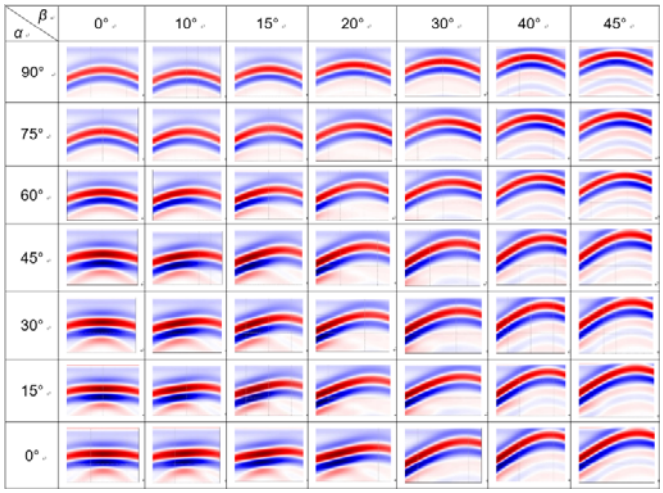

Fig. 4 Images of simulated data in different situations.

III. Results

A. *Effects Of Root Orientation On The Reflecting Signal's Shape And In Situ Identification*

Fig.4 shows the alteration of the angle between the root and the GPR survey line lead to the change in the shape of the B-scan. Actually, the horizontal angle α and the vertical inclination β can influence respectively the shape of the hyperbolae. Obviously, the hyperbolae become more and more flatter when the α diminishes (from the top to the bottom in Fig.4. Likely, as β increase, the asymmetry of hyperbolae appears more and more clearly. Furthermore, the coordinate information of hyperbolic vertex has been acquired by the symmetry algorithm as shown in Fig.5 , of course, it can be seen that the position of hyperbolic vertex tended to higher with the increment of β in Fig.4. As shown in the Fig.5, to facilitate the use of the algorithm, we remove the direct wave in GPR hyperbolae by Matgpr3.0. Also the essential information of hyperbolae vertex can be inversion by symmetry algorithm and Hough algorithm. As shown in Fig.5, the blue part respectively express scanning number (n) and the echo time delay (t) as well as the relative error that can reflect the accuracy of data to large extent are shown in the white part. The scanning number is influenced by the α and β, so the hyperbolic vertex coordinates calculated by inversion data are expressed as:

$$X_0 = n \times \Delta x + d$$
$$Y_0 = v \cdot t \quad (12)$$

Where the Δx denotes the space step of the radar scanning, and the d denotes the spacing between the transmitting antenna and the receiving antenna. V is the electromagnetic wave velocity and t is shown in Fig.4.

As well as, the coordinate of hyperbolae vertex calculated by the forward model can using following equation:

$$X_1 = x + (h - y) \times \sin\beta \times \cos\beta \times \cos\alpha \quad (13)$$

In (13).x and y respectively denotes the horizontal and vertical coordinates of the center of the root. As well as the h is the height of GPR.

Compared to x, the calculation formula of y is much simpler. The inversion coordinate of y is the product of time delay and wave velocity. The theory coordinate of y can be expressed as:

$$Y_1 = (h - y) \times \sin 2\beta \quad (14)$$

The effect on the hyperbola is also reflected in the symmetry curve as shown in Fig.6. In an ordinary way, symmetry algorithm can directly reflect the degree of symmetry of hyperbola. The x-coordinate of the curve will shift to the right as β goes from 0° to 45°,in the meantime, it also became increasingly asymmetrical. However, under the same β, there is almost no difference in the scan position at the vertex of a hyperbola. In conclusion, the regularity of symmetry curve and hyperbola is one - to - one correspondence.

There is another index that more directly reflects the change in the hyperbola vertex, that is the coordinates numerical. Only we gain the velocity of the electromagnetic wave, can we get the coordinate of the vertex of the hyperbola. With the help of the Hough Transform Algorithm, we get the value of V (0.001) in the Fig.3(b). As shown in the Table 1, this table summarized the data collected during the experiment of the inversion. To make it more intuitive, the abscissa is represented by the number of scan channels of the radar directly above the root, while the vertical axis is shown in millimeters. Obviously, the abscissa of hyperbolic vertex is affected by horizontal angle and vertical inclination, similarly, the ordinate of hyperbolic vertex is influenced by vertical inclination β. In addition to the coordinates of these targets, the relative error (the white box shown in figure 5) also can provided a more comprehensive data interpretation.

In fact, in order to recognize coarse roots in situ, we combine the hough transform with the symmetry algorithm, which is a simple and typical. On the other hand, the reflection hyperbola of the root contains a lot of information, so that we can just use the random hough transform to automatically recognize the hyperbola, but that's a later story.

Overall, the results have proven that the positions of the hyperbolic vertex will move as the change of the root direction. In our study, to some extent, we can discern the signal of root

reflection hyperbola although the in situ recognition of root is affected by a number of factors.

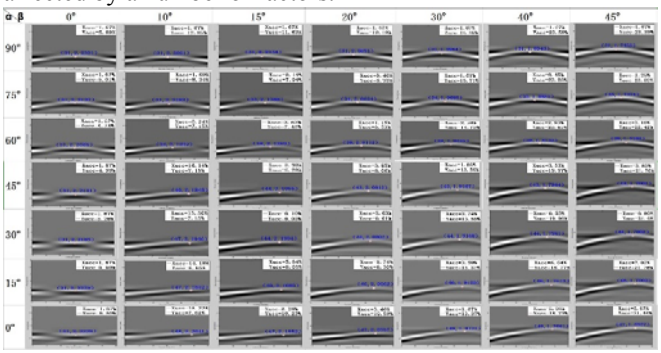

Fig. 5 The coordinate inversion in different root directions and relative error calculation

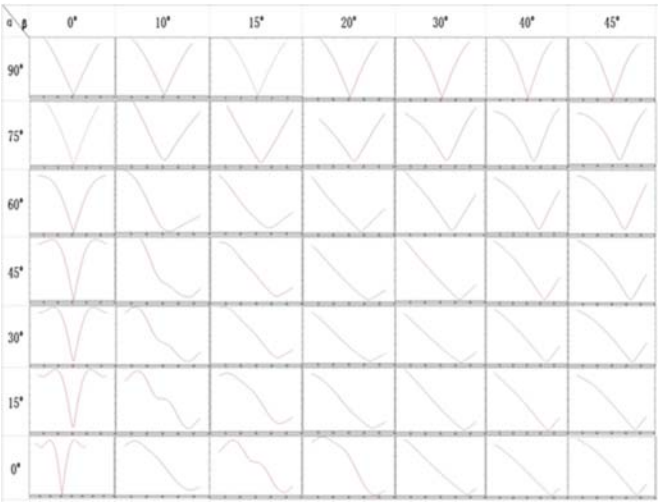

Fig. 6 The symmetry curve of the hyperbola of GPR in 49 root directions.

B. Detection Of Root Hyperbola In Simulation Experiment And Field Experiment

To illustrate the quality of the recognition results of the algorithm, we applied the above detection algorithm to the simulation experiment and field experiment [36-37]. Fig.7 and Fig.8 show the result of detection in the GPR image. In the Fig.8, the feature points are represented by red and green dots. The vertices of the hyperbola are marked with red dots, while the two wings of the hyperbola is indicated by green dots. Thus we can identify the vertex position and curve contour of the GPR hyperbola. Then, as shown in the right side of Fig.7, we can draw the outline of the hyperbola. In each figure, the hyperbola contour and the vertex position are not identical because of the complexity of roots growing underground. As shown in the Fig.8, we set up four detection circles that is respectively 0.3m, 0.45m, 0.6m and 0.75m. A detection circle indicates that the GPR goes around the tree in the specified radius. If there's something underground that's different from the permittivity of the soil, a hyperbola will be produce. Of course, there is no root if not have a hyperbola in GPR image. Furthermore, the Fig.8 shows root reflected signal in four detection circles that a circle around the tree, the red box is the hyperbola of the root. A notable question is there are many hyperbolics, but not always a reflection of the root. Because the underground is particularly complex that includes lots of cracks, pipes, foreign matters and so on.

Table 1: GPR hyperbola vertex coordinates in 49 root directions.

α \ β	0°	10°	15°	20°	30°	40°	45°
90°	(31, 7. 1469)	(31, 7. 3638)	(31, 7. 0924)	(31, 6. 6858)	(31, 6. 3853)	(31, 6. 0618)	(31, 5. 5849)
75°	(31, 7. 0838)	(31, 7. 0986)	(33, 6. 84416)	(34, 6. 5997)	(34, 6. 2992)	(35, 6. 0419)	(35, 5. 5597)
60°	(31, 7. 0672)	(34, 7. 0237)	(38, 6. 8125)	(38, 6. 4358)	(38, 6. 2256)	(39, 5. 8022)	(39, 5. 5034)
45°	(31, 7. 0819)	(46, 7. 0234)	(44, 6. 7376)	(43, 6. 4038)	(43, 6. 1334)	(43, 5. 7421)	(43, 5. 4403)
30°	(31, 7. 0992)	(47, 7. 0227)	(44, 6. 7213)	(44, 6. 4001)	(44, 6. 1338)	(44, 5. 7411)	(44, 5. 4406)
15°	(31, 7. 1133)	(47, 6. 9926)	(45, 6. 7216)	(46, 6. 4198)	(46, 6. 1184)	(46, 5. 6361)	(46, 5. 4401)
0°	(31, 7. 1133)	(48, 7. 6557)	(49, 6. 2845)	(47, 6. 7062)	(48, 6. 1338)	(48, 5. 6515)	(47, 5. 4102)

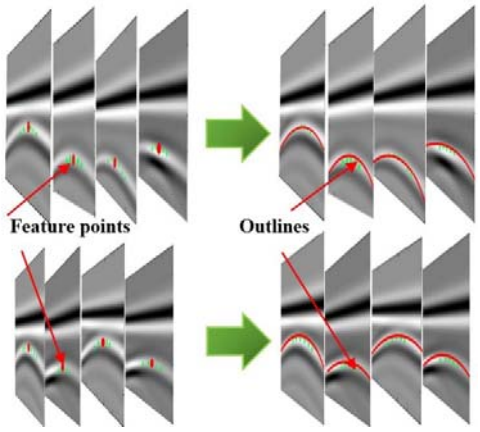

Fig. 7 Hyperbola vertex discern of forward models and identification of hyperbolic contour

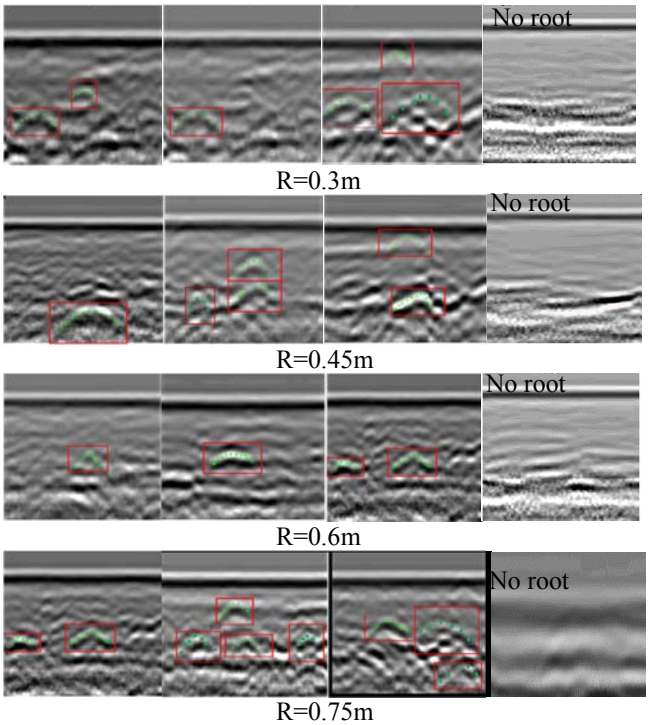

Fig.8 The GPR reflection images of root in the four detection circles, respectively are 0.3m, 0.45m, 0.6m and 0.75m.

On the other hand, if we determine that the hyperbola is produced by the root system, we can draw them in three dimensions based on their location. That is to say three-dimensional reconstruction of root systems. Three-dimensional root reconstruction is a huge task, the detection of the hyperbola is just a small part of it.

IV. Discussion and Conclusion

Previous studies are focused on the root biomass detection, the automatic 3D reconstruction of roots, and has made a lot of achievements. However, it still exist many factors that affect the results of GPR detection in these processes, such as center frequency of GPR, the diameter, the dielectric constant, the moisture content of the root and so on. That is to say what we are doing is only one aspect. Though these factors restrict the detection of root to some extent, our research still has significant science value. It's worth mentioning that the coarse root is use to experiment because coarse roots are easier to detect than thin roots.

This study elaborated the effect of root direction on the hyperbola of GPR signal, the main aim of the research was to provide effective and high-precision location of tree root systems. For this purpose, we put forward a feasible algorithm for locating root systems based on two different algorithms. In different directions of single root growth, we summarize the change rule of hyperbola vertex with root direction and get its coordinates relative error. In the end, we propose a part of 3d reconstruction of root systems. There is no doubt that it provides a foundation for future 3d reconstruction.

However, coordinate inversion of root systems is more or less inaccurate because our hyperbola model is idealized. As shown in Fig.5, the relative error in the horizontal and vertical coordinates averages less than 20 percent. And the relative error of the ordinate is generally greater than that of the abscissa. In addition, the accuracy of the results is limited by many factors, such as, the GPR frequency, the radius of roots, the moisture content of soil and roots and so on. As for the practicability of this paper, we will continue to do further research.

REFERENCES

[1] Ma Z, Guo D, Xu X, et al. Evolutionary history resolves global organization of root functional traits[J]. Nature, 2018, 555, 94-+.

[2] Leatherman S P. Coastal Geomorphological Applications of Ground-Penetrating Radar [J]. Journal of Coastal Research, 1987, 3(3):397-399.

[3] Victor S N, Sonia S A, Pérez-Gracia Vega. GPR Clutter Amplitude Processing to Detect Shallow Geological Targets[J]. Remote Sensing, 2018, 10(2):88-.

[4] Gao L , Jie Y , Ning L , et al. Dielectric Characteristics of Unsaturated Loess and the Safety Detection of the Road Subgrade Based on GPR[J]. Journal of Sensors, 2018, 2018:1-8.

[5] Hruska J. Mapping tree root systems with ground-penetrating radar[J]. Tree Physiol. 1999, 19.

[6] Frédéric Danjon, Reubens B. Assessing and analyzing 3D architecture of woody root systems, a review of methods and applications in tree and soil stability, resource acquisition and allocation[J]. Plant and Soil, 2008, 303(1-2):1-34.

[7] Cui X H, Chen J, Shen J S, et al. Modeling tree root diameter and biomass by ground-penetrating radar[J]. Science in China Series D: Earth Sciences, 2011, 54(5):711-719.

[8] Meng Liu, Liang Ma, Na Wang, et al. Passive multiple target indoor localization based on joint interference cancellation in an RFID System[J]. Electronics 2019, 8, 426.

[9] Leucci G. The use of three geophysical methods for 3D images of total root volume of soil in urban environments[J]. Exploration Geophysics, 2011, 41.

[10] Birken R, Miller DE, Burns M. Efficient Large-Scale Underground Utility Mapping with a Multi-Channel Ground-Penetrating Imaging Radar System[J]. SPIE 2002, 4758, 186-191.

[11] Doolittle J A, Bellantoni N F. The search for graves with ground-penetrating radar in Connecticut[J]. Journal of Archaeological Science, 2010, 37(5):0-949.

[12] Liu K N, Yang Q L, Sun Y J, et al. 3D Reconstruction of Jatropha curcas L. Root Based on Image[J]. Advanced Materials Research, 2012.

[13] Zhu S, Huang C, Su Y, et al. 3D Ground Penetrating Radar to Detect Tree Roots and Estimate Root Biomass in the Field[J]. Remote Sensing, 2014, 6(6):5754-5773.

[14] Yokota Y, Matsumoto M, Gaber A, et al. Estimation of biomass of tree roots by GPR with high accuracy positioning system[C]// Geoscience & Remote Sensing Symposium. IEEE, 2011.

[15] Guo L, Lin H, Fan B, et al. Impact of root water content on root biomass estimation using ground penetrating radar: evidence from forward simulations and field controlled experiments[J]. Plant and Soil, 2013, 371(1-2):503-520.

[16] Molon M, Boyce J, I Arain. Quantitative, non-destructive estimates of coarse root biomass in a temperate pine forest using 3-D ground-penetrating radar (GPR)[J]. Journal of Geophysical Research 2017, 122, 80-102.

[17] Butnor J R, Doolittle J A, Johnsen K H, et al. Utility of Ground-Penetrating Radar as a Root Biomass Survey Tool in Forest Systems[J]. Soil Science Society of America Journal, 2003, 67(5):1607.

[18] Dannoura M, Hirano Y, Igarashi T, et al. Detection of\r, Cryptomeria japonica\r, roots with ground penetrating radar[J]. Plant Biosystems - An International Journal Dealing with all Aspects of Plant Biology, 2008, 142(2):375-380.

[19] Fang S, Yan X, Liao H. 3D reconstruction and dynamic modeling of root architecture in situ and its application to crop phosphorus research[J]. Plant Journal for Cell & Molecular Biology, 2010, 60(6):1096-1108.

[20] Wu Y, Guo L, Cui X, et al. Ground-penetrating radar-based automatic reconstruction of three-dimensional coarse root system architecture[J]. Plant and Soil, 2014, 383(1-2):155-172.

[21] Liu Q, Cui X, Liu X, et al. Detection of Root Orientation Using Ground-Penetrating Radar[J]. IEEE Transactions on Geoscience and Remote Sensing, 2017, PP(99):1-12.

[22] Barton C V M, Montagu K D. Detection of tree roots and determination of root diameters by ground penetrating radar under optimal conditions[J]. Tree Physiology, 2004, 24(12):1323-1331.

[23] Hirano Y, Dannoura M, Aono K, et al. Limiting factors in the detection of tree roots using ground-penetrating radar[J]. Plant and Soil, 2009, 319(1-2):15-24.

[24] Reubens, B.; Poesen, J.; Danjon, F.; Geudens, G.; Muys, B. The role of fine and coarse roots in shallow slope stability and soil erosion control with a focus on root system architecture: a review. Trees-Struct. Funct. 2007, 21, 385–402.

[25] Reubens B, Poesen J, Frédéric Danjon, et al. The role of fine and coarse roots in shallow slope stability and soil erosion control with a focus on root system architecture: a review[J]. Trees -, Structure and Function, 2007, 21(4):385-402.

[26] LaiFernOw, EngKoonSim. Detection of urban tree roots with the ground penetrating radar[J]. Giornale botanico italiano, 2012, 146(sup1):10.

[27] Wentao L, Xihong C, Li G, et al. Tree Root Automatic Recognition in Ground Penetrating Radar Profiles Based on Randomized Hough Transform[J]. Remote Sensing, 2016, 8(5):430-.

[28] Butnor J R, Doolittle J A, Kress L, et al. Use of ground-penetrating radar to study tree roots in the southeastern United States[J]. Tree Physiology, 2001, 21(17):1269-1278.

[29] Guo L, Lin H, Fan B, et al. Forward simulation of root's ground penetrating radar signal: simulator development and validation[J]. Plant and Soil, 2013, 372(1-2):487-505.

[30] Yuan D, Fan D. Salient map of hyperbolas in GPR images[J]. EURASIP Journal on Image and Video Processing, 2018, 2018(1).
[31] Huang C L, Chen C W. Human facial feature extraction for face interpretation and recognition[J]. Pattern Recognition, 1992, 25(12):1435-1444.
[32] Mertens L, Persico R, Matera L, et al. Automated Detection of Reflection Hyperbolas in Complex GPR Images With No A Priori Knowledge on the Medium[J]. IEEE Transactions on Geoscience and Remote Sensing, 2015:1-17.
[33] Prasad V S N, Yegnanarayana B. Finding Axes of Symmetry From Potential Fields[J]. IEEE Transactions on Image Processing, 2004, 13(12):1559-1566.
[34] Tzanis, Andreas. Detection and extraction of orientation-and-scale-dependent information from two-dimensional GPR data with tuneable directional wavelet filters[J]. Journal of Applied Geophysics, 2013, 89:48-67.
[35] Holbrook W S, Miller S N, Provart M A. Estimating snow water equivalent over long mountain transects using snowmobile-mounted ground-penetrating radar[J]. Geophysics, 2016, 81(1):WA183-WA193.
[36] Zhou H L, Wan X T, Xiang L. Subsurface cylindrical object location and material inversion from GPR data-based online SVR[J]. Nondestructive Testing Communications, 2014, 29(1):13.
[37] Alnuaimy W, Huang Y, Nakhkash M, et al. Automatic detection of buried utilities and solid objects with GPR using neural networks and pattern recognition[J]. Journal of Applied Geophysics, 2000, 43(2):157-165.